Human–machine shared control for vehicle lane keeping systems: a Lyapunov-based approach

Chouki Sentouh, Tran Anh-Tu Nguyen, Jagat Jyoti Rath, Jérôme Floris, Jean-christophe Popieul

IET Intelligent Transport Systems

Special Issue: Recent Advancements on Electrified, Low Emission and Intelligent Vehicle-Systems

IET Journals
The Institution of Engineering and Technology

Human–machine shared control for vehicle lane keeping systems: a Lyapunov-based approach

ISSN 1751-956X
Received on 31st March 2018
Revised 2nd July 2018
Accepted on 7th August 2018
E-First on 12th October 2018
doi: 10.1049/iet-its.2018.5084
www.ietdl.org

Chouki Sentouh[1], Anh-Tu Nguyen[1], Jagat Jyoti Rath[1] ✉, Jérôme Floris[1], Jean-Christophe Popieul[1]

[1]LAMIH, CNRS, UMR 8201, Campus du Mont Houy, F-59313 Valenciennes, France

✉ *E-mail: jagatjyoti.rath@gmail.com*

Abstract: In this work, a human-centred steering assist controller based on dynamic allocation of control authority between driver and automatic e-copilot has been proposed for lane keeping systems. Cooperative control between driver and steering assist controller is addressed taking into consideration human driving behaviour. The vehicle steering controller for lane keeping is designed using a driver model for representation of the conflict between the driver and the controller. The steering controller is designed employing the integrated driver-vehicle model using Takagi–Sugeno control technique coupled with Lyapunov stability tools. The proposed design is robust to longitudinal speed variations and involves a trade-off between the lane following performance and ratio of negative system interference. The proposed approach was implemented on dynamic vehicle simulator SHERPA and the results presented in this study demonstrate the effectiveness of the proposed structure for cooperative control action between human driver and the steering assistance system. Based on indices such as energies spent by driver, driver satisfaction level and contradiction level between driver and autonomous controller the proposed optimal approach shows 93.48% and 89.30% reductions in expended driver energy and contradiction levels. Further, the satisfaction level of driver increased by 67.80% while performing a lane change manoeuvre.

1 Introduction

Advanced driver assistance systems (ADASs) have been the focus of active research in public institutions and the industry in recent years. With varying areas of application, category and type, these systems can be categorised broadly on the basis of level of automation, interaction with human driver, area of application [1–3]. The design of advanced, intelligent and efficient ADASs such as lane keeping assist (LKA), adaptive cruise control, collision avoidance and so on have been carried out in many works and successfully implemented. However, the successful integration of these systems in the control design while taking into consideration the human driver and thereby cooperatively controlling the vehicle remains a challenging topic of research [4, 5]. Prior research indicates that use of intelligent transportation system approaches in vehicles could have a negative impact on safety and driving performance unless they are integrated so as to work in cooperation with the driver [6, 7].

The design of a human-centred intelligent vehicle is characterised by the coordinating system [8] that monitors the cooperative activity between the driver and the automation system. In the absence of a coordinating system, the vehicle is subject to various overlapping or conflicting scenarios without any cooperation between driver and automation having a common goal [9]. In this work, the lateral motion control of a vehicle considering cooperative action is addressed. Thus, in the aspect of lateral control, it can be said that the driver and the steering controller perform actions to steer the vehicle for a specific driving task while having control of vehicle simultaneously. In such a scenario, the driver and the e-copilot (i.e. steering controller) share the objectives and representation of the driving task, environment and so on to ensure there is no negative interference between them while having a good situation awareness of the effective dynamic control allocation [10, 11]. In the previous works on the ADAS systems, the necessity of an active coordination between the human driver and the automation system [2, 6, 12, 13] has been highlighted to avoid the negative interference.

Steering angle control based lateral motion regulation of a vehicle has been addressed in various approaches such as [14–16]. The use of steering angle provides a better robustness because the loop of the steering wheel angle control algorithm allows to compensate the non-linearity of the steering system. In the above works, the control action was applied as an additional steering angle to the driver input. However, the steering angle based approach fails to consider the intervention of the driver on the steering process and such controllers replace the driver in performing the driving task. For cooperative control, driver-in-the-loop design and effective steering torque control are required. The work in [17] addressed a procedure for the design of lane-keeping control that uses steering torque as control input using a full state feedback with $\mathscr{H}_2$ control theory. However, in the design process of the controller, the driver torque was considered as disturbance input and no coordination of the authority between human driver and controller was considered. The effective coordination of the authority between the driver and a steering assist controller was addressed in [13] where a robust adaptive steering controller was developed to provide steering correction that can compensate the difference between the human driver and an *idealised* driver model. The conflict between the steering assist controller and the human driver was handled using a switching rule based on a difference between the controller and the driver actions. Similarly in [18], automatic lane-keeping in combination with driver's steering for either obstacle avoidance or lane-change manoeuvres using a 2-DOF control strategy was discussed. The control was always active with the advantage that no on/off switching strategy was used. When the driver steered the steering wheel, the vehicle motion was controlled by the driver through the vehicle steering system and when there was no driver's steering action, the automatic lane-keeping system ensured the lane keeping. However, this control strategy could ensure only manual or automatic steering modes and there was no shared lateral control mode possible.

To achieve higher levels of performance, the design of active safety systems that can share responsibility with human driver, must integrate a minimum of understanding of the driver behaviour (actions and intentions) and also information about the driving environment [19]. Subsequently, cooperative LKA strategies based on H_2 control, Takagi–Sugeno (T–S) fuzzy control, $\mathscr{H}_\infty$ control were proposed in [4, 20–22]. In these works, driver models were integrated with the vehicle dynamics to formulate a driver-in-the loop model and cooperative control architectures were designed. In

Table 1 Vehicle nomenclature

Notation	Description
M	mass of vehicle, kg
C_f/C_r	cornering stiffness of the front/rear tires, N/rad
I_z	moment inertia about the yaw axis, kgm^2
l_f/l_r	distances of the front/rear tire from CG, m
l_w	lateral wind force impact distance, m
l_s	look-ahead distance, m
f_w	lateral wind force, N
v_x/v_y	vehicle longitudinal/lateral speed, m/s
r	vehicle yaw rate, rad/s
ψ_L	relative yaw angle, rad
y_L	lateral offset from the centreline, m
c_x/c_y	longitudinal/lateral aerodynamic drag coefficient, dimensionless
I_s	moment of inertia of the steering system, kgm^2
I_{eff}	effective longitudinal inertia, kgm^2
B_s	damping coefficient of the steering system, Nm/rad/s
R_s	reduction ratio of the steering system, dimensionless
η_t	width of the tire contact, m
$T_a/T_d/T_{al}$	assistance/driver/self-aligning torque, Nm

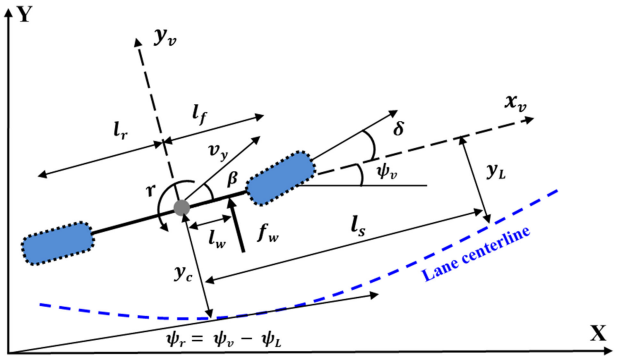

Fig. 1 *Lateral vehicle behaviour modelling*

a similar line, in this paper we extend our previous work in [3] for the design of a novel cooperative control architecture for a driver-in-the-loop model based on a structural driver model, using optimal control theory that guarantees robustness and stability. The contribution of this paper is to propose a design methodology of the human-centred driving assistance system where the human driver and the electronic copilot can cooperatively drive together.

The shared control combines several objectives which may be conflicting in some cases, such as the accuracy of lane following and the intrusiveness level with the driver. The goal is to meet these objectives while preserving the system stability to improve the interaction between the driver and the assistance. To this end, we have introduced a driver model for designing a T–S optimal controller to allow a representation of the conflict between the driver and the controller in the quadratic criterion, by considering the weighting of the driver torque and that of the controller. This new concept allows to resolve conflicting driving situations in order to successfully share lateral control of the vehicle between human driver and controller. The assistance shall not reject the driver action and not consider it as a disturbance. The control authority shifting between the driver and the steering controller is designed by introducing a decision-making algorithm to manage the intervention module in order to select the corresponding control strategy according to the driving situation. The system can be parameterised to be activated only when an absence of the driver action on the steering wheel is detected which contributes to avoid road departure crashes due to driver fatigue after a long-time driving. The main contributions of the paper can be summarised as follows:

- A new driver-in-the-loop vehicle model is proposed for shared control design which can manage the conflict issue between the human driver and the LKA system.
- A dynamic control allocation strategy based on the idea of optimal control is proposed to ensure cooperative lane keeping control while minimising system interference.
- Based on Lyapunov stability arguments, we reformulate the design of shared steering controller as an linear matrix inequality LMI-based optimisation problem which can be effectively solved with available numerical solvers [23]. The effectiveness of the proposed shared control approach is clearly proved with experimental validations on a dynamic vehicle simulator.

The paper is organised as follows. In Section 2, we present the dynamic vehicle and driver models used for designing the simulation scenarios and the lane keeping controller. Section 3 presents and discusses the design process of the lane keeping controller. The control authority shifting between the human driver and the steering assist controller is then investigated. The experimental results and evaluations of the shared control performance are discussed in Section 4. Section 5 concludes the paper and provides the future works.

2 Vehicle and driver modelling

This section presents the modelling of both the vehicle dynamics and the driver lane keeping behaviour. The vehicle nomenclature is given in Table 1.

2.1 Non-linear vehicle model

To investigate the vehicle lateral motions, the non-linear single-track model is used to represent the vehicle handling dynamics in the horizontal plane [24, 25] (see Fig. 1). To this end, the vehicle dynamics can be described as follows [24]:

$$\begin{aligned}\dot{v}_x &= \frac{T_{\text{eng}} - c_x v_x^2}{I_{\text{eff}}} + v_y r \\ \dot{v}_y &= \frac{F_{yf} + F_{yr} - c_y v_y^2 + f_w}{M} - v_x r \\ \dot{r} &= \frac{1}{I_z}(l_f F_{yf} - l_r F_{yr} + l_w f_w)\end{aligned} \tag{1}$$

where T_{eng} is the net engine/brake torque which is the control input for the vehicle longitudinal dynamics. The cornering forces at the front tires F_{yf} and rear tires F_{yr} are, respectively, modelled using the well-known *magic* formula [26]

$$\begin{aligned}F_{yi}(\alpha_i) &= \mathscr{D}_i \sin(\nabla_i) \\ \nabla_i &= \mathscr{C}_i \arctan[(1-\mathscr{E}_i)\mathscr{B}_i\alpha_i + \mathscr{E}_i \arctan(\mathscr{B}_i\alpha_i)]\end{aligned} \tag{2}$$

where $i \in \{f, r\}$. The Pacejka parameters $\mathscr{B}_i$, $\mathscr{C}_i$, $\mathscr{D}_i$ and $\mathscr{E}_i$ in (2) depend on the characteristics of the tire, road and the vehicle operating conditions [26]. The sideslip angles for the front and rear tires are given by

$$\alpha_f = \delta - \arctan\left(\frac{v_y + l_f r}{v_x}\right), \quad \alpha_r = \arctan\left(\frac{v_y - l_r r}{v_x}\right) \tag{3}$$

where δ is the steering angle. For lateral control purposes, the non-linear vehicle (1) is further simplified in the sequel.

2.2 Road-vehicle control-based model

In this paper, we focus on the shared lateral control in normal driving conditions of intelligent vehicles. As a result, the following assumptions can be considered [27]:

- The dynamics of the longitudinal speed v_x and the aerodynamic forces are neglected.

- The lateral tire forces are proportional to the slip angles of each axle, i.e. linear pseudo-slip behaviour.
- The steering angle δ is assumed to be small.

Note that the relevance of these assumptions for normal driving has been shown in various lateral control contexts (see for instance [4, 21, 27, 28]). As a consequence, the lateral forces at the front and rear tires are modelled by

$$F_{yf} = C_f\alpha_f = C_f\left(\delta - \frac{v_y + l_f r}{v_x}\right),$$
$$F_{yr} = C_r\alpha_r = -C_r\left(\frac{v_y - l_r r}{v_x}\right).$$

Therefore, the linear vehicle lateral dynamics is given as follows [28]:

$$\begin{bmatrix}\dot{v}_y\\ \dot{r}\end{bmatrix} = \begin{bmatrix}a_{11} & a_{12}\\ a_{21} & a_{22}\end{bmatrix}\begin{bmatrix}v_y\\ r\end{bmatrix} + \begin{bmatrix}b_1\\ b_2\end{bmatrix}\delta + \begin{bmatrix}e_1\\ e_2\end{bmatrix}f_w \tag{4}$$

where

$$a_{11} = \frac{-2(C_r + C_f)}{Mv_x}, \quad a_{12} = -v_x + \frac{2(l_r C_r - l_f C_f)}{Mv_x},$$
$$a_{21} = \frac{2(l_r C_r - l_f C_f)}{I_z v_x}, \quad a_{22} = \frac{-2(l_r^2 C_r + l_f^2 C_f)}{I_z v_x}, \tag{5}$$
$$b_1 = \frac{2C_f}{M}, \quad b_2 = \frac{2l_f C_f}{I_z}, \quad e_1 = \frac{1}{M}, \quad e_2 = \frac{l_w}{I_z}.$$

To represent the road-vehicle positioning, the following dynamics of the heading error ψ_L and the lateral offset y_L from the road centreline at a look-ahead distance are incorporated into the vehicle system (see Fig. 1)

$$\begin{aligned}\dot{\psi}_L &= r - \rho_r v_x\\ \dot{y}_L &= v_y + l_s r + \psi_L v_x\end{aligned} \tag{6}$$

where ρ_r is the road curvature. The vehicle steering system is modelled in order to consider the driver feeling to the steering torque feedback and the assistance one. The steering system dynamics is given as follows [20]:

$$I_s R_s \ddot{\delta} = T_d + T_a - T_{al} \tag{7}$$

where the self-aligning torque is given by

$$T_{al} = \frac{2C_f\eta_t}{R_s}\left(\delta - \frac{v_y + l_f r}{v_x}\right) - R_s B_s \dot{\delta}.$$

From (4), (6) and (7), the linear road-vehicle model with steering system can be represented in the following form:

$$\dot{\boldsymbol{x}}_v = \boldsymbol{A}_v\boldsymbol{x}_v + \boldsymbol{B}_v(T_a + T_d) + \boldsymbol{D}_v\boldsymbol{w} \tag{8}$$

where $\boldsymbol{x}_v^\top = \begin{bmatrix}v_y & r & \psi_L & y_L & \delta & \dot{\delta}\end{bmatrix}$ is the vehicle state vector, and $\boldsymbol{w}^\top = \begin{bmatrix}f_w & \rho_r\end{bmatrix}$ is the disturbance of the vehicle system. The system matrices in (8) are given by

$$\boldsymbol{A}_v = \begin{bmatrix}a_{11} & a_{12} & 0 & 0 & b_1 & 0\\ a_{21} & a_{22} & 0 & 0 & b_2 & 0\\ 0 & 1 & 0 & 0 & 0 & 0\\ 1 & l_s & v_x & 0 & 0 & 0\\ 0 & 0 & 0 & 0 & 0 & 1\\ T_{s_1} & T_{s_2} & 0 & 0 & T_{s_3} & T_{s_4}\end{bmatrix}, \quad \boldsymbol{B}_v = \begin{bmatrix}0\\ 0\\ 0\\ 0\\ 0\\ \frac{1}{I_s R_s}\end{bmatrix},$$
$$\boldsymbol{D}_v = \begin{bmatrix}e_1 & e_2 & 0 & 0 & 0 & 0\\ 0 & 0 & -v_x & 0 & 0 & 0\end{bmatrix}^{\mathrm{T}}$$

where

$$T_{s1} = \frac{2\eta_t C_f}{I_s R_s^2 v_x}, \quad T_{s2} = \frac{2l_f\eta_t C_f}{I_s R_s^2 v_x},$$
$$T_{s3} = \frac{-2\eta_t C_f}{I_s R_s^2}, \quad T_{s4} = \frac{-B_s}{I_s}.$$

For the vehicle system (8), the driver torque T_d is measured whereas the assistance torque T_a has to be designed such that the studied LKA system can effectively share the vehicle control with the human driver.

2.3 Driver-vehicle model for shared steering control

In order to manage the conflict between the human driver and the LKA system, the driver dynamics should be incorporated into the vehicle system for driver-in-the-loop control purposes. With the focus on lane keeping control, here the driver model used for shared control design is proportional to the lateral deviation error observed by the driver and the heading error

$$T_d = k_{d1}y_d + k_{d2}\psi_L \tag{9}$$

where

$$y_d = v_y + l_d r + \psi_L v_x, \quad l_d = T_p v_x.$$

The preview time T_p is a dynamic entity affected by vehicle speed, road curvature and the driver's path view strategy. In general, a higher speed requires longer preview time for vehicle stability and tends to decrease considerably with increase in road curvature. In addition, the preview time depends on the speed influence assuming constant driving speed within the preview interval. However, depending on the type of driver model chosen, the impact of the variation of v_x on preview time is significantly different. Various researches [28–30] have pointed, based on experimental studies, that the range of preview time is between [0.5 s, 1.5 s]. It is of note that that the minimisation of the heading error requires a high preview time and any deviation from the real driver preview time generates an under-steering (i.e. $T_p < T_p$of driver) or oversteering (i.e. $T_p > T_p$of driver). In this work, considering general real-world driving scenarios, we have considered the preview time of 1 s. In previous works of our group [20, 31–33], multiple tests with various driver data were conducted and the influence of preview time for different driving tasks has been evaluated. Based on such tests, in this work a standard preview time of 1 s has been considered in this work for the development of the shared architecture. The driver torque dynamics can be directly derived from (9) as

$$\dot{T}_d = k_{d1}v_y + \left(k_{d1}T_p v_x + k_{d2}\right)r + k_{d1}v_x\psi_L - k_{d2}v_x\rho_r \tag{10}$$

From (8) and (10), the global driver-road-vehicle system can be represented in the form

$$\dot{\boldsymbol{x}} = \boldsymbol{A}\boldsymbol{x} + \boldsymbol{B}\boldsymbol{u} + \boldsymbol{D}\boldsymbol{w} \tag{11}$$

where $\boldsymbol{x} = \begin{bmatrix} x_v & T_d \end{bmatrix}^\top$ and $\boldsymbol{u} = T_a$. The state-space matrices of (11) are given by

$$\boldsymbol{A} = \begin{bmatrix} \boldsymbol{A}_v & \boldsymbol{B}_v \\ \boldsymbol{E} & 0 \end{bmatrix}, \quad \boldsymbol{B} = \begin{bmatrix} \boldsymbol{B}_v \\ \boldsymbol{0} \end{bmatrix}, \quad \boldsymbol{D} = \begin{bmatrix} \boldsymbol{D}_v \\ \boldsymbol{F} \end{bmatrix}, \tag{12}$$

with $\boldsymbol{E} = \begin{bmatrix} a_{71} & a_{72} & a_{73} & 0 & 0 & 0 \end{bmatrix}$, $\boldsymbol{F} = \begin{bmatrix} 0 & -k_{d2}v_x \end{bmatrix}$, $a_{71} = k_{d1}$, $a_{72} = k_{d1}T_p v_x + k_{d2}$ and $a_{73} = k_{d1}v_x$. We note that the dynamics of (11) depends *explicitly* on the time-varying vehicle speed. To improve the shared control performance under various driving situations, we propose in the next section a Lyapunov-based control method taking into account this time-varying parameter dependency.

3 T–S fuzzy approach for shared steering control

This section presents the design of shared steering controller between the human driver and the LKA system. The control approach is based on an *exact* T–S fuzzy representation of the driver-vehicle system using Lyapunov stability arguments.

3.1 Shared control specifications

The multiple objectives of lane tracking, driver comfort enhancement and conflict minimisation are now incorporated into the shared control design. To account for lane tracking, the deviation errors (via y_L and ψ_L) require to be minimised. Similarly, the driver comfort is assessed based on the limits of lateral acceleration (a_y) and the steer rate ($\dot{\delta}$) similar to the works [4, 5, 20–22]. To address the issue of conflict, we introduce the difference between the driver and assist torque, i.e. $T_d - T_a$ as a factor to be minimised. For a typical manoeuvre, if the driver and autonomous system are in conflict, the torques generated by them are in opposite directions. The conflict level between the two systems can then be analysed as a measure of the resistance to the driver from the assistance system. To minimise that, the factor $T_d - T_a$ is considered as a performance output for the proposed T–S fuzzy optimal controller and hence reduce the effects of negative interference from the assisting system. The performance output of the driver-vehicle system (11) is then defined

$$z = \begin{bmatrix} \psi_L & y_L & a_y & \dot{\delta} & T_d - T_a \end{bmatrix}^\top \tag{13}$$

Subsequently, the controlled output z in (13) can be rewritten in the following form:

$$z = \boldsymbol{G}\boldsymbol{x} + \boldsymbol{H}\boldsymbol{u} \tag{14}$$

where

$$\boldsymbol{G} = \begin{bmatrix} 0 & 0 & 1 & 0 & 0 & 0 & 0 \\ 0 & 0 & 0 & 1 & 0 & 0 & 0 \\ a_{11} & a_{12} + v_x & 1 & 0 & b_1 & 0 & 0 \\ 0 & 0 & 0 & 0 & 0 & 1 & 0 \\ 0 & 0 & 0 & 0 & 0 & 0 & 1 \end{bmatrix}, \quad \boldsymbol{H} = \begin{bmatrix} 0 \\ 0 \\ 0 \\ 0 \\ -1 \end{bmatrix}.$$

3.2 T–S representation of driver-vehicle system

The state-space and the performance matrices of (11) depend on both speed terms v_x and $\vartheta_x = 1/v_x$ which are measured and bounded as

$$v_{\min} \le v_x \le v_{\max}, \quad v_{\min} = 5,\ \text{m/s}, \quad v_{\max} = 25\,\text{m/s}\,. \tag{15}$$

To make clear this parameter dependency feature, we rewrite the driver-vehicle system (11) and its performance vector (14) in the following form:

$$\begin{cases} \dot{\boldsymbol{x}} = \boldsymbol{A}(\theta)\boldsymbol{x} + \boldsymbol{B}\boldsymbol{u} + \boldsymbol{D}(\theta)\boldsymbol{w} \\ z = \boldsymbol{G}(\theta)\boldsymbol{x} + \boldsymbol{H}\boldsymbol{u} \end{cases} \tag{16}$$

where $\theta = \begin{bmatrix} v_x & \vartheta_x \end{bmatrix}^\top$. Using the sector non-linearity approach in [34], the driver-vehicle model (16) can be *exactly* represented as follows:

$$\begin{cases} \dot{\boldsymbol{x}} = \sum_{i=1}^{4} h_i(\theta)(\boldsymbol{A}_i\boldsymbol{x} + \boldsymbol{B}_i\boldsymbol{u} + \boldsymbol{D}_i\boldsymbol{w}) \\ z = \sum_{i=1}^{4} h_i(\theta)(\boldsymbol{G}_i\boldsymbol{x} + \boldsymbol{H}_i\boldsymbol{u}) \end{cases} \tag{17}$$

where $\boldsymbol{B}_i = \boldsymbol{B}$, $\boldsymbol{H}_i = \boldsymbol{H}$, for $i \in \{1, \ldots, 4\}$, and

$$\begin{aligned} &\boldsymbol{A}_1 = \boldsymbol{A}(v_{\min}, \vartheta_{\min}), && \boldsymbol{G}_1 = \boldsymbol{G}(v_{\min}, \vartheta_{\min}), \\ &\boldsymbol{A}_2 = \boldsymbol{A}(v_{\min}, \vartheta_{\max}), && \boldsymbol{G}_2 = \boldsymbol{G}(v_{\min}, \vartheta_{\max}), \\ &\boldsymbol{A}_3 = \boldsymbol{A}(v_{\max}, \vartheta_{\min}), && \boldsymbol{G}_3 = \boldsymbol{G}(v_{\max}, \vartheta_{\min}), \\ &\boldsymbol{A}_4 = \boldsymbol{A}(v_{\max}, \vartheta_{\max}), && \boldsymbol{G}_4 = \boldsymbol{G}(v_{\max}, \vartheta_{\max}) \\ &\boldsymbol{D}_1 = \boldsymbol{D}(v_{\min}), && \boldsymbol{D}_2 = \boldsymbol{D}(v_{\min}), \\ &\boldsymbol{D}_3 = \boldsymbol{D}(v_{\max}), && \boldsymbol{D}_4 = \boldsymbol{D}(v_{\max})\,. \end{aligned}$$

The membership functions in (17) are defined as

$$\begin{aligned} h_1(\theta) &= \Omega_1(\theta) \cdot \Theta_1(\theta), \quad h_2(\theta) = \Omega_1(\theta) \cdot \Theta_2(\theta), \\ h_3(\theta) &= \Omega_2(\theta) \cdot \Theta_1(\theta), \quad h_4(\theta) = \Omega_2(\theta) \cdot \Theta_2(\theta), \end{aligned} \tag{18}$$

where

$$\begin{aligned} \Omega_1(\theta) &= \frac{v_{\max} - v_x}{v_{\max} - v_{\min}}, \quad \Omega_2(\theta) = \frac{v_x - v_{\min}}{v_{\max} - v_{\min}}, \\ \Theta_1(\theta) &= \frac{\vartheta_{\max} - \vartheta_x}{\vartheta_{\max} - \vartheta_{\min}}, \quad \Theta_2(\theta) = \frac{\vartheta_x - \vartheta_{\min}}{\vartheta_{\max} - \vartheta_{\min}}\,. \end{aligned} \tag{19}$$

It is worth noting that the scalar membership functions satisfy the following property [34]:

$$\sum_{i=1}^{r} h_i(\theta) = 1, \quad h_i(\theta) \ge 0, \quad \forall i \in \{1, \ldots, 4\} \tag{20}$$

The convex sum property (20) is used hereafter to derive tractable LMI-based control design conditions.

3.3 T–S fuzzy model-based control design

For control design, we make use of the following parameter-dependent state feedback controller:

$$\boldsymbol{u} = \sum_{i=1}^{4} h_i(\theta)\boldsymbol{K}_i\boldsymbol{x} = K(\theta)\boldsymbol{x} \tag{21}$$

and a Lyapunov function of the quadratic form

$$V(x) = \boldsymbol{x}^\top \boldsymbol{P}^{-1}\boldsymbol{x}, \quad \boldsymbol{P} > \boldsymbol{0} \tag{22}$$

We consider the following control problem.

Problem 1: Determine the feedback gains $\boldsymbol{K}_i$, $i \in \{1, \ldots, 4\}$, and the Lyapunov function (22) such that the controller (21) stabilises the closed-loop system (17) while minimising the following performance index:

$$\mathcal{J} = \int_0^\infty (z^\top \mathcal{Q} z + u^\top \mathcal{R} u)\,\mathrm{d}t, \quad x(0) = 0 \tag{23}$$

where $\mathcal{Q} = \mathrm{diag}[q_{\psi_L} \quad q_{y_L} \quad q_{a_y} \quad q_{\dot{\delta}} \quad q_{T_d}]$ and $\mathcal{R}$ are positive definite weighting matrices which should be appropriately chosen for shared lateral control purposes.

The following theorem provides an LMI-based solution for Problem 1.

Theorem 1: Given the driver-vehicle system (17). If there exist a positive definite matrix $\boldsymbol{P}$, matrices $\boldsymbol{N}_i$, for $i \in \{1, \ldots, 4\}$ of appropriate dimensions and a positive scalar γ satisfying the following optimisation:

$$\min_{\xi_i, i \in \{1,\ldots,4\}} \gamma \tag{24}$$

$$\text{subject to} \tag{25}$$

$$\begin{bmatrix} \Phi_i & \star & \star & \star \\ G_i P + H N_i & -\mathcal{Q}^{-1} & \star & \star \\ N_i & 0 & -\mathcal{R}^{-1} & \star \\ D_i^{\mathrm{T}} & 0 & 0 & -\gamma I \end{bmatrix} < 0 \tag{26}$$

where $\xi_i = (\gamma, \boldsymbol{P}, \boldsymbol{N}_i)$, $\boldsymbol{\Phi}_i = \boldsymbol{A}_i\boldsymbol{P} + \boldsymbol{B}\boldsymbol{N}_i + (\boldsymbol{A}_i\boldsymbol{P} + \boldsymbol{B}\boldsymbol{N}_i)^{\mathrm{T}}$ and the symbol $\star$ stands for matrix blocks that can be deduced by symmetry. Then, the control law (21) with the feedback gains defined as follows:

$$\boldsymbol{K}_i = \boldsymbol{N}_i\boldsymbol{P}, \quad i \in \{1, \ldots, 4\} \tag{27}$$

solves Problem 1.

Proof: Refer Appendix. □

Remark 1: The control design in Theorem 1 is formulated as a convex optimisation problem under LMI constraints. The feedback gains $\boldsymbol{K}_i$, for $i \in \{1, \ldots, 4\}$, can be easily computed using Matlab software with YALMIP toolbox [35].

It is important to note that by applying Theorem 1 to the augmented model (11) for shared steering control design, we obtain feedback gains K_i composed by two parts:

$$\boldsymbol{u} = \sum_{i=1}^{r} h_i(\theta)(\boldsymbol{K}_{Ei}\boldsymbol{x}_v + K_{\Gamma i}T_d) \tag{28}$$

The first part $\boldsymbol{K}_{Ei}$ can ensure the lane keeping performance whereas the second part $K_{\Gamma i}$ aims to modulate the driver action on the steering wheel. In the absence of the driver torque ($T_d = 0$), the system reacts as an autonomous LKA system. In the presence of the driver torque, the system assists the human driver to do what he/she desires when the vehicle error positioning is small. However, when the vehicle drifts from the centre of the lane, the controller counteracts the driver to bring the vehicle back to the centre of the lane.

4 Experimental results and discussions

This section presents some partial experimental results obtained using the dynamic driving SHERPA simulator which includes a Peugeot 206 car and three projection screens supporting 270° of sight. The setup consists of a full car mock-up equipped with CAN bus to perform various hardware-in-the loop experiments. The SHERPA vehicle simulator represented in Fig. 2 is equipped with an active steering wheel with a sensor providing steering angle, steering rate sensor and steering torque (see Fig. 2). The SHERPA-LAMIH simulator uses the software SCANeR and offers the possibility to use RTMaps and Matlab/Simulink development environments. The SHERPA simulator has been employed to perform various tests related to vehicle road safety such as driver state (fatigue, drowsiness etc.) detection, driver workload assessment, driver biomechanical behaviour assessment and so on. For more specific details on the SHERPA simulator, refer [36]. Multiple tests for driver identification have been conducted using the SHERPA simulator. The detailed results for validation of driver models have been presented in [20, 31–33]. Employing similar identification procedures, the driver parameters for the proposed model (9) were identified as $k_{d1} = -4.5852$ and $k_{d2} = -59.4173$.

Fig. 2 *SHERPA: dynamic LAMIH driving simulator (left), steering torque sensor (right)*

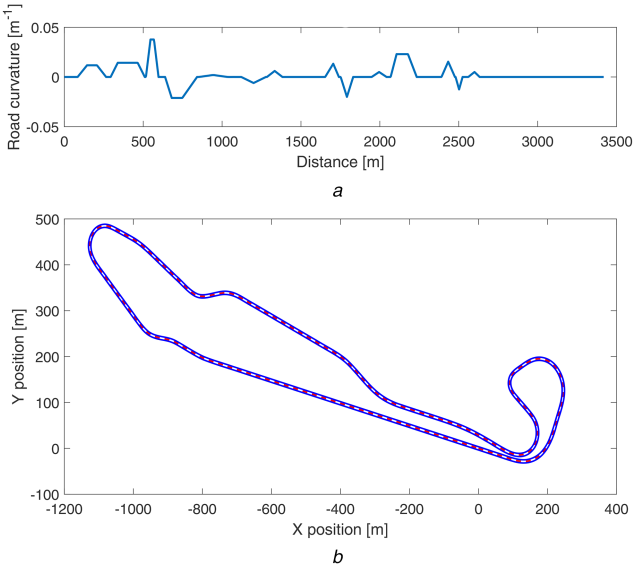

Fig. 3 *Satory test track*
(a) Road curvature of satory test track, ***(b)*** Satory test track X-Y positions

4.1 Lane following manoeuvre

In this section, the proposed T–S LKA controller which integrates a driver model in the design process of the control law is tested for lane following manoeuvre with and without driver interaction. The digital database of the Satory test track polled in Fig. 3*b* is used for the simulations with the road curvature polled in Fig. 3*a*. The vehicle speed is fixed at $v = 15$ m/s.

In the first test, the steering of the vehicle is performed only by the controller to ensure the vehicle lane keeping in order to evaluate robustness of the synthesised controller when the vehicle drives in a curved road. From Figs. 4 and 5, we can note that the controller reacts well to the road curvature disturbance through a torque applied to the steering column system. Figs. 5*a* and *b* show, respectively, the lateral deviation and heading error and illustrate the good lane keeping performance of the proposed steering controller. Fig. 5 shows the trajectory performed by the vehicle and we can see that the vehicle remains on the road during the driving test. For the second test, we consider the shared control mode where both driver and controller are in action and the vehicle steering is performed both by the driver and the LKA controller. It can be noticed from Fig. 6 that the designed controller gives to the driver a certain freedom to operate according to his driving style and the control is shared between the driver and the assistance as can be seen in Fig. 6*c*. We can notice according to Fig. 6 that the steering controller provides about 50% of the required torque without generating negative interference and no conflict situation has been detected in this case. In this experiment, the driver performs an overtaking manoeuvre to avoid an obstacle on the road which is not specified to the controller. The overtaking manoeuvre is started by the driver from time $t = 76$ s to $t = 86$ s as shown in Fig. 6*a* where the lateral deviation error reaches 3.4 m.

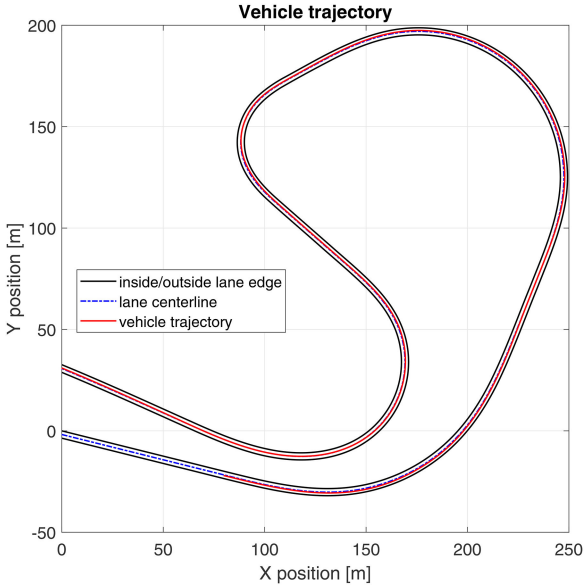

Fig. 4 *Test of the lane following manoeuvre*

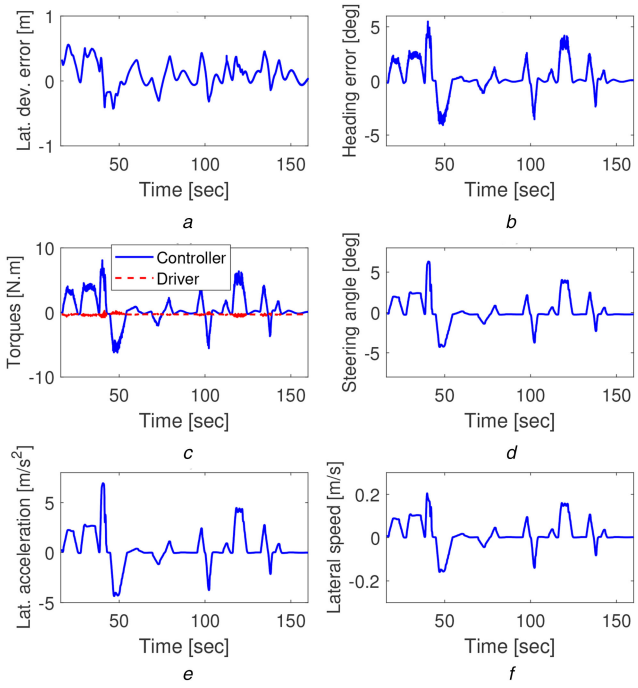

Fig. 5 *Test of the lane following manoeuvre: automatic control*
(a) Lateral deviation error, ***(b)*** Heading error, ***(c)*** Torques applied, ***(d)*** Steering wheel angle, ***(e)*** Lateral acceleration, ***(f)*** Lateral speed

4.2 Lane change manoeuvre

We now examine the interaction between the driver and the LKA system when the driver overrides the system to perform a lane change manoeuvre or overtaking. In this experiment, the vehicle is supposed to be on a straight road section with vehicle speed fixed at $v_x = 15$ m/s. The designed driver model-based T–S optimal LKA controller (LKCDM) is compared to the classical one synthesised considering only the vehicle model (8) without considering a driver/controller conflict management (LKWDM). The driver and controller torques in the case of manual driving, shared control with LKCDM controller and shared control with LKWDM are plotted, respectively, in Figs. 7*a*–*c*. As it can be seen, the proposed LKCDM controller has a behaviour similar to an electric power assisted steering system where the driver is assisted to achieve his desired steering manoeuvre. However, using the LKWDM, the controller torque is opposite to the driver one during overtaking manoeuvres as it can be seen in Fig. 7*c*. This means that a negative interference is generated because the driver's action on

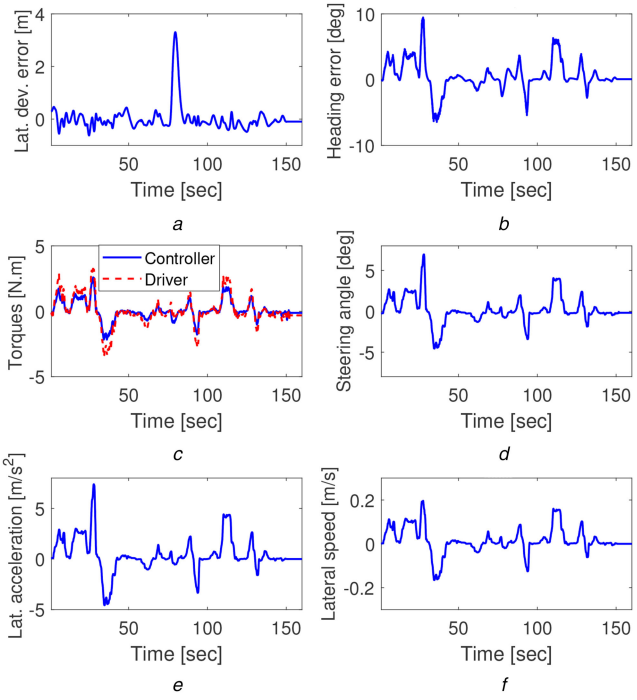

Fig. 6 *Test of the lane following manoeuvre: shared control*
(a) Lateral deviation error, ***(b)*** Heading error, ***(c)*** Torques applied, ***(d)*** Steering wheel angle, ***(e)*** Lateral acceleration, ***(f)*** Lateral speed

the steering wheel is regarded by the controller as a disturbance to reject. When we use the LKCDM controller, it is possible to consider this negative interference minimisation as a control law objective and thus the controller adapts its action according to the driver action. The controller gives to the driver a certain freedom to operate according to his driving style and thus the control is shared between driver and assistance as can be seen in Fig. 7*b*. This figure shows that the steering of the vehicle is performed both by the driver and the controller which provides about 40% of the required torque, without generating negative interference. The lateral displacement of the vehicle during the overtaking manoeuvre is plotted in Fig. 7*d*.

In order to test the robustness of the LKCDM controller against longitudinal speed, we test a lane following performance with longitudinal speed variation and overtaking manoeuvres with different speeds, 60 and 90 km/h. Fig. 8 illustrates the dynamic response of the vehicle during the overtaking manoeuvres with $v_x = 60$ and $v_x = 90$ km/h. We can see from this figure that the yaw rate r and the lateral acceleration a_y remain in the comfort range.

4.3 Performance evaluation

In this section, we evaluated the achieved performance for both lane following and lane change manoeuvres by calculating the maximum absolute value of the lateral deviation error $|y_{cg}|_{\max}$ and the maximum absolute value of the heading error $|\psi_L|_{\max}$. The feeling of the driver is evaluated by the calculation of the effort devoted by him (the energy of the steering torque signal) and by the controller ($E_{\{c,d\}}$) to perform a driving task in a time interval $[t_1, t_2]$ such as

$$E_{\{c,d\}} = \int_{t_1}^{t_2} T_{\{c,d\}}^2(t)\,\mathrm{d}t \tag{29}$$

We also introduce a parameter that is called a degree of satisfaction for the lane change manoeuvre (i.e. during an obstacle avoidance) given by [20]

$$W_d = \frac{\int_{t_1}^{t_2} y_{cg}(t)\,\mathrm{d}t}{E_d(t_1, t_2)} \tag{30}$$

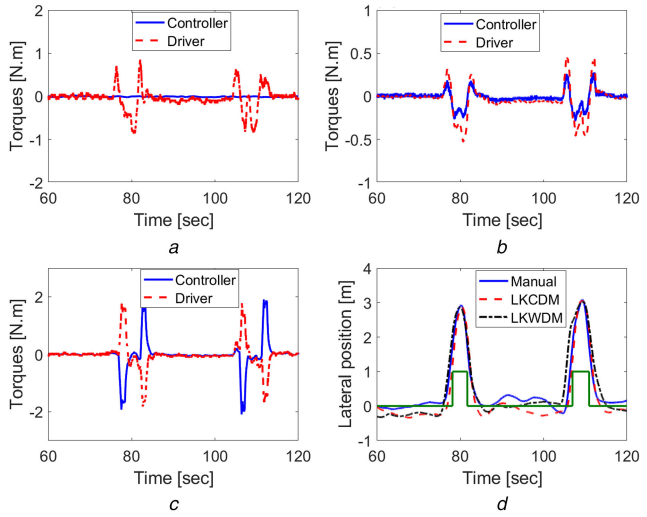

Fig. 7 *Test of the overtaking manoeuvre*

(a) Manual driving, ***(b)*** Shared control with LKCDM, ***(c)*** Shared control with LKWDM, ***(d)*** Lateral displacement

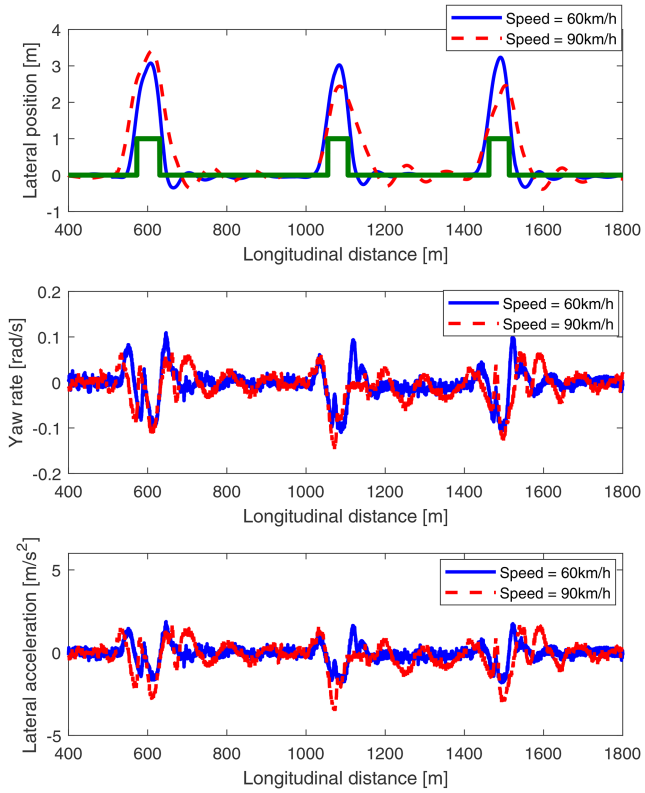

Fig. 8 *Test of the overtaking manoeuvre*

The contradiction level between the driver action and that of the assistance during the lane change manoeuvre is also analysed based on the cosine of the angle between the driver and assistance torque vectors (dot product) which characterises the direction of the two vectors [4]

$$\theta_{\text{con}} = \cos^{-1}\left(\frac{T_c \cdot T_d}{\| T_c \| \cdot \| T_d \|}\right) \tag{31}$$

A comparison of lane following performance of the two designed controllers LKCDM and LKWDM and the sharing quality of the tests performed in the first four turns of the Satory test track (see Fig. 3 and Fig. 9) is summarised in Table 2. It can be deduced from the presented results that both lane errors, i.e. y_L and ψ_L have low values for the proposed controller. It can also be deduced that in the scenario when shared control without the driver model was evaluated, the energy expended by the driver and the automation

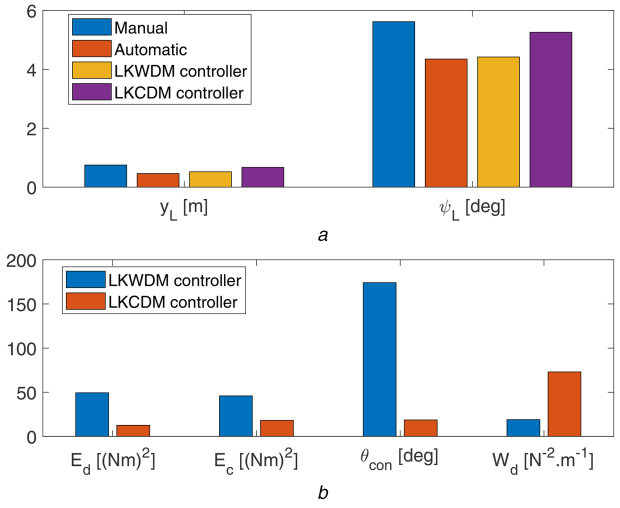

Fig. 9 *Performance evaluation*

(a) Lane following performance, ***(b)*** Conflict level performance during overtaking manoeuvre

Table 2 Comparison of the lane following performance

Test	Performance index			
	$\|y_L\|_m$ (m)	$\|\psi_1\|$ (deg)	E_c, (Nm^2)	E_d, (Nm^2)
manual	0.75	5.62	—	279.27
auto	0.46	4.35	276.92	—
S-LKWDM	0.52	4.42	185.72	34.57
S-LKCDM	0.67	5.26	154.07	18.20

system were 87.62 and 32.93% lower than the manual driving and autonomous driving scenarios, respectively. However, for the driver-in-the-loop design proposed in this paper, the energies spent are 93.48 and 44.36% lower than the manual driving and autonomous driving scenarios, respectively, which is much lower than the previous scenario. This justifies that with the driver-in-the-loop approach proposed in this work, lane keeping performance of the vehicle is maintained with less effort from the driver and the automation system. Consequently, Table 3 summarises the different computed indicators characterising the driver/controller interaction during a double lane change manoeuvre to avoid an obstacle. From Table 3, the proposed optimal approach results in 61.18% reduction in energy for the driver in comparison to the human driver. However, for the case where driver model was not used there is an increase in the energy spent by the driver by 51.95%. This is reflected in the degree of satisfaction values for both cases. Hence, in the LKCDM the value of W_d deteriorates by 23.73% while in the LKCDM case, W_d increases by 67.80% in comparison to the manual driving scenario. Further, the contradiction levels analysed using θ_{con} show that in the proposed optimal approach, the contradiction between driver and autonomous controller drops by 89.30%. Thus, the overall performance of the proposed approach can be easily deduced from the presented results showing minimisation of conflict while ensuring lane tracking.

5 Conclusions

In this paper, a novel cooperative control approach for lane keeping system based on a robust optimal control strategy was proposed. To evaluate the cooperative action, a driver-in-the-loop model was developed by integrating the vehicle lateral dynamics with a driver model based on lane errors. The proposed optimal control strategy was designed based on T–S fuzzy approach to ensure minimal lane deviation errors, improve driver comfort and reduce the interference from the system. The proposed design was experimentally validated on the dynamic SHERPA vehicle simulator for different driving scenarios such as lane following, obstacle avoidance and so on. Extensive results to show the performance of the proposed scheme in comparison with

Table 3 Comparison of conflict level during overtaking manoeuvre

Test	Performance index				
	E_d, (Nm^2)	E_c, (Nm^2)	$\|y_L\|_m$, (m)	W_d	θ_{con}
manual	32.51	—	3.95	59	—
S-LKWDM	49.40	45.91	3.46	19	174.11
S-LKCDM	12.62	18.19	3.25	73	18.63

autonomous controller, shared control without a driver model and manual driver have been presented to show the robustness. It was established that employing the proposed scheme the energy spent by the driver for a particular task is reduced when considering a driver-in-the-loop design by 93.48% in comparison to the manual driving scenario. Further, the reduction in interference from the autonomous controller to the driver for the proposed optimal strategy was shown while the vehicle navigated an obstacle avoidance scenario. It was found that the driver satisfaction level increased by 67.80% and the contradiction level dropped by 89.30% using the proposed approach.

6 Acknowledgments

This work has been done within the framework of the AutoConduct project (ANR-16-CE22-0007), funded by the Agence Nationale de la Recherche. This work was also supported by the International Campus on Safety and Intermodality in Transportation, the Hauts-de-France Region, the European Community, the Regional Delegation for Research and Technology, the Ministry of Higher Education and Research, and the French National Center for Scientific Research.

7 References

[1] Inagaki, T.: 'Adaptive automation: sharing and trading of control', *Handbook Cognit. Task Des.*, 2003, **8**, pp. 147–169
[2] Flemisch, F., Schieben, A., Kelsch, J., *et al.*: 'Automation spectrum, inner/outer compatibility and other potentially useful human factors concepts for assistance and automation', *Human Factors Assist. Autom.*, 2008, pp. 1–16
[3] Sentouh, C., Debernard, S., Popieul, J.-C., *et al.*: 'Toward a shared lateral control between driver and steering assist controller', *IFAC Proc.*, 2010, **43**, (13), pp. 404–409
[4] Saleh, L., Chevrel, P., Claveau, F., *et al.*: 'Shared steering control between a driver and an automation: stability in the presence of driver behavior uncertainty', *IEEE Trans. Intell. Transp. Syst.*, 2013, **14**, (2), pp. 974–983
[5] Schnelle, S., Wang, J., Su, H., *et al.*: 'A driver steering model with personalized desired path generation', *IEEE Trans. Syst. Man Cyber., Syst.*, 2017, **47**, (1), pp. 111–120
[6] Bainbridge, L.: 'Ironies of automation', *Automatica*, 1983, **19**, (6), pp. 775–779
[7] Clegg, C., Gray, M., Waterson, P.: 'The charge of the byte brigade and a socio-technical response', *Int. J. Hum.-Comput. Stud.*, 2000, **52**, (2), pp. 235–251
[8] Li, L., Wen, D., Zheng, N.-N., *et al.*: 'Cognitive cars: A new frontier for ADAS research', *IEEE Trans. Intell. Transp. Syst.*, 2012, **13**, (1), pp. 395–407
[9] Woods, D., Roth, E., Bennett, K.: 'Cognition, computing, and cooperation', in Robertson, S.P., Zachary, W.W., Black, J.B. (Eds): '*Ch. Explorations in joint human-machine cognitive systems*' (Ablex Publishing Corp., Norwood, NJ, USA, 1990), pp. 123–158
[10] Hoc, J.-M., Debernard, S.: 'Respective demands of task and function allocation on human-machine cooperation design: A psychological approach', *Connect. Sci.*, 2002, **14**, (4), pp. 283–295
[11] Debernard, S., Guiost, B., Poulain, T., *et al.*: 'Integrating human factors in the design of intelligent systems: An example in air traffic control', *Int. J. Intell. Syst. Technol. Appl.*, 2009, **7**, (2), pp. 205–226
[12] Biester, L.: 'The concept of cooperative automation in cars: results from the experiment overtaking on highways'. 3rd Int. Driving Symp. Human Factors Driver. Assessment, Training, and Vehicle Design, Rocksport, ME, USA, 2005, pp. 342–348
[13] Chen, L.-K., Shieh, B.-J.: 'Coordination of the authority between the vehicle driver and a steering assist controller', *WSEAS Trans. Syst. Control*, 2008, **3**, (5), pp. 353–364
[14] Netto, M., Chaib, S., Mammar, S.: 'Lateral adaptive control for vehicle lane keeping'. American Control Conf., Boston, Massachusetts, USA, 2004, vol. 3, pp. 2693–2698
[15] Peng, H.: 'Evaluation of driver assistance systems: a human centered approach'. Proc. 6th Symp. Advanced Vehicle Control, Hiroshima, Japan, 2002
[16] Falcone, P., Ali, M., Sjoberg, J.: 'Predictive threat assessment via reachability analysis and set invariance theory', *IEEE Trans. Intell. Transp. Syst.*, 2011, **12**, (4), pp. 1352–1361
[17] Shimakage, M., Satoh, S., Uenuma, K., *et al.*: 'Design of lane-keeping control with steering torque input', *JSAE Soc. Autom. Eng. Japan*, 2002, **23**, (3), pp. 317–323
[18] Cerone, V., Milanese, M., Regruto, D.: 'Combined automatic lane-keeping and driver's steering through a 2-DOF control strategy', *IEEE Trans. Control Syst. Technol.*, 2009, **17**, (1), pp. 135–142
[19] Goodrich, M., Boer, E.: 'Designing human-centered automation: trade-offs in collision avoidance system design', *IEEE Trans. Intell. Transp. Syst.*, 2000, **1**, (1), pp. 40–54
[20] Soualmi, B., Sentouh, C., Popieul, J., *et al.*: 'Automation-driver cooperative driving in presence of undetected obstacles', *Control Eng. Pract.*, 2014, **24**, pp. 106–119
[21] Nguyen, A.-T., Sentouh, C., Popieul, J.-C.: 'Driver-automation cooperative approach for shared steering control under multiple system constraints: design and experiments', *IEEE Trans. Ind. Electron.*, 2017, **64**, (5), pp. 3819–3830
[22] Wang, W., Xi, J., Liu, C., *et al.*: 'Human-centered feed-forward control of a vehicle steering system based on a driver's path-following characteristics', *IEEE Trans. Intell. Transp. Syst.*, 2017, **18**, (6), pp. 1440–1453
[23] Boyd, S., El Ghaoui Feron, L., *et al.*: '*Linear matrix inequalities in system and control theory*', vol. 15 (SIAM, Philadelphia, 1994)
[24] Swaroop, D., Yoon, S.M.: 'The design of a controller for a following vehicle in an emergency lane change maneuver'. Tech. Rep. UCB-ITS-PWP-99-3, February 1999, University of California
[25] Nguyen, A.-T., Chevrel, P., Claveau, F.: 'On the effective use of vehicle sensors for automatic lane keeping via LPV static output feedback control', *IFAC-PapersOnLine*, 2017, **50**, (1), pp. 13808–13815, 20th IFAC World Congress
[26] Pacejka, H.: '*Tire and vehicle dynamics*' (Elsevier, Butterworth-Heinemann, Oxford, UK, 2005)
[27] Enache, N., Netto, M., Mammar, S., *et al.*: 'Driver steering assistance for lane departure avoidance', *Control Eng. Pract.*, 2009, **17**, (6), pp. 642–651
[28] Rajamani, R.: '*Vehicle dynamics and control*' (Springer, US, 2012)
[29] Taheri, S.: 'Steering control characteristics of human driver coupled with an articulated commercial vehicle'. PhD dissertation, Concordia University, 2014
[30] Yashimoto, K.: 'Simulation of driver/vehicle system including preview control', *J. Mech. Soc. Japan*, 1968, **7**
[31] Pick, A.J., Cole, D.J.: 'A mathematical model of driver steering control including neuromuscular dynamics', *J. Dyn. Syst. Meas. Control*, 2008, **130**, (3), pp. 1–9
[32] Sentouh, C., Nguyen, A.T., Benloucif, M.A., *et al.*: 'Driver-automation cooperation oriented approach for shared control of lane keeping assist systems', *IEEE Trans. Control Syst. Technol.*, 2018, DOI: 10.1109/TCST.2018.2842211
[33] Guo, C., Sentouh, C., Popieul, J.C., *et al.*: 'Predictive shared steering control for driver override in automated driving: a simulator study', *J. Transp. Res. F, Psychol. Behav.*, 2018, DOI: 10.1016/j.trf.2017.12.005
[34] Tanaka, K., Wang, H.: '*Fuzzy control systems design and analysis: a linear matrix inequality approach*' (Wiley-Interscience, New York, NY, USA, 2004)
[35] Löfberg, J.: 'YALMIP: A toolbox for modeling and optimization in MATLAB'. IEEE Int. Symp. Computer-Aided Control Systems Design, Taipei, 2004, pp. 284–289
[36] SHERPA: Available at www.univ-valenciennes.fr/LAMIH/en/SHERPA

8 Appendix

8.1 Proof of Theorem 1

Since the membership functions satisfy (20), multiplying (26) by $h_i(\theta) \geq 0$ and summing up for all $i \in \{1, \ldots, 4\}$, we obtain clearly that

$$\begin{bmatrix} \Phi(\theta) & \star & \star & \star \\ G(\theta)\boldsymbol{P} + HN(\theta) & -\mathscr{Q}^{-1} & \star & \star \\ N(\theta) & 0 & -\mathscr{R}^{-1} & \star \\ D(\theta)^{\top} & 0 & 0 & -\gamma I \end{bmatrix} < 0 \tag{32}$$

where $N(\theta) = \sum_{i=1}^{4} h_i(\theta) N_i$ and

$$\Phi(\theta) = \sum_{i=1}^{4} h_i(\theta)\left(A_i\boldsymbol{P} + \boldsymbol{B}\boldsymbol{N}_i + (A_i\boldsymbol{P} + \boldsymbol{B}\boldsymbol{N}_i)^{\top}\right)$$
$$= \boldsymbol{A}(\theta)\boldsymbol{P} + \boldsymbol{B}N(\theta) + (\boldsymbol{A}(\theta)\boldsymbol{P} + \boldsymbol{B}N(\theta))^{\top}$$

Applying successively two times the well-known Schur complement lemma [23] to (32), it follows that

$$\begin{bmatrix} \Upsilon(\theta) + N(\theta)^{\top}\mathscr{R}N(\theta) & \star \\ D(\theta)^{\top} & -\gamma I \end{bmatrix} < 0 \tag{33}$$

where

$$\Upsilon(\theta) = \Phi(\theta) + (G(\theta)\boldsymbol{P} + HN(\theta))^{\top}\mathscr{Q}(G(\theta)\boldsymbol{P} + HN(\theta))$$

It follows easily from (27) that $N(\theta) = K(\theta)\boldsymbol{P}^{-1}$. Then, pre- and post-multiplying (33) with the diagonal block-matrix $\mathrm{diag}(\boldsymbol{P}^{-1}, I)$ leads to

$$\begin{bmatrix} \Psi(\theta) + K(\theta)^{\top}\mathscr{R}K(\theta) & \star \\ D(\theta)^{\top}P^{-1} & -\gamma I \end{bmatrix} < 0 \tag{34}$$

where

$$\Psi(\theta) = P^{-1}(\boldsymbol{A}(\theta) + \boldsymbol{B}K(\theta)) + (\boldsymbol{A}(\theta) + \boldsymbol{B}K(\theta))^{\top}\boldsymbol{P}^{-1}$$
$$+(G(\theta) + HK(\theta))^{\top}\mathscr{Q}(G(\theta) + HK(\theta)).$$

Pre- and post-multiplying (34) with the vector $[\boldsymbol{x} \quad w]$, we obtain the following Hamilton-Jacobi inequality after some simple algebraic manipulations:

$$\dot{V}(x) + z^{\top}\mathscr{Q}z + u^{\top}\mathscr{R}u < \gamma w^{\top}w \tag{35}$$

where $\dot{V}(x)$ is the time derivative of the Lyapunov function (22) along the trajectory of (17). The inequality (35) implies $\dot{V}(x) < \gamma w^{\top}w$. This guarantees the stability of the disturbed system (17). Moreover, integrating both sides of (35) while considering $x(0) = 0$, we obtain easily that

$$\int_0^{\infty} (z^{\top}\mathscr{Q}z + u^{\top}\mathscr{R}u)\,\mathrm{d}t < \gamma\,|w|_2^2 \tag{36}$$

Observe in (36) that by minimising γ, we minimise the performance index $\mathscr{J}$ defined in (23). This concludes the proof.